Primljen / Received: 17.10.2017.
Ispravljen / Corrected: 30.1.2019.
Prihvaćen / Accepted: 10.8.2023.
Dostupno online / Available online: 10.11.2023.

Influence of earthquake angle on seismic performance of concrete highway bridges

Authors:

Prof. **Ahmet Can Altunışık**, PhD. CE
Karadeniz Technical University, Trabzon, Turkey
Department of Civil Engineering
ahmetcan8284@hotmail.com
Corresponding author

Ebru Kalkan Okur, PhD. CE
Karadeniz Technical University, Trabzon, Turkey
Department of Civil Engineering
ebrukalkan@ktu.edu.tr

Professional paper

Ahmet Can Altunışık, Ebru Kalkan Okur

Influence of earthquake angle on seismic performance of concrete highway bridges

This study aims to evaluate the effect of earthquake angle on the seismic performance of a concrete highway bridge. As a numerical example, a twin prestressed concrete box-girder highway bridge was analysed using finite element methods. The bridge was subjected to the 1992 Erzincan earthquake ground accelerations in 19 directions with values ranging from 0° to 90° in 5-degree increments. To evaluate the effects of different earthquake angles on seismic performance, variations in the maximum displacements, internal forces and principal stresses on the bridge deck, columns, isolator and foundation were studied . The results changed considerably for different earthquake angles. Variations in the displacement, internal forces and principal stresses occurred at different incidence angles. In other words, there is no unique angle of incidence for each structure.

Key words:
concrete highway bridge, earthquake angle influence, finite element method, seismic performance

Stručni rad

Ahmet Can Altunışık, Ebru Kalkan Okur

Utjecaj kuta djelovanja potresa na seizmičko ponašanje betonskih mostova na autocestama

Cilj je ovog istraživanja procijeniti učinak kuta djelovanja potresa na seizmičko ponašanje betonskog mosta na autocesti. Analiziran je dvostruki prednapeti betonski sandučasti gredni most na autocesti (odvojena konstrukcija za svaki smjer vožnje) kao numerički primjer i to primjenom metode konačnih elemenata. Most je bio izložen djelovanju potresa ubrzanja tla u Erzincanu iz 1992. i to u 19 smjerova čije vrijednosti variraju od 0 ° do 90 ° s povećanjima od 5 stupnjeva. Kako bi se ispitali učinci različitih kutova djelovanja potresa na seizmičku izvedbu, proučene su promjene vrijednosti maksimalnih pomaka, unutarnjih sila te glavnih naprezanja na kolničku konstrukciju mosta, stupova, izolatora i temelja. Rezultati su se znatno promijenili u slučaju različitih kutova djelovanja potresa. Pojavile su se promjene vrijednosti pomaka, unutarnjih sila i glavnih naprezanja pri različitim upadnim kutovima. Drugim riječima, ne postoji jedinstveni upadni kut za svaku konstrukciju.

Ključne riječi:
betonski most na autocesti, utjecaj kuta djelovanja potresa, metoda konačnih elemenata, seizmička izvedba

1. Introduction

In many different designs made from various construction materials, bridges are used by pedestrians and vehicles as a normal part of our daily lives. Damage to bridges through the dynamic load effect of earthquakes can have huge physical and financial consequences for communities and many intangible side effects. This effect is known to vary considerably with variations in the earthquake angle. Many studies have examined this effect and described the most extreme conditions.

Earthquake ground motions have three components with different intensities, including two orthogonal components in the lateral and vertical directions; in general, all design codes suggest that the two lateral earthquake components should be perpendicular to each other [1-3]. According to EN 1998-2 [1], the probable maximum action affects E owing to the simultaneous occurrence of the components of the seismic action along the horizontal axes X-Y and the vertical axis Z, which may be estimated through the application of the SRSS rule to the maximum action effects Ex, Ey, and Ez owing to independent seismic action along each axis. In many analysis programs, the directions of the earthquake forces are applied by default. When the angles of the earthquake directions were changed such that the angle between the X-, Y-, and Z is 90o, the displacement and internal forces formed in each element of the structure were significantly affected. Analytical formulae have been used for many years to determine the critical angle of earthquake ground motion. From these equations, the maximum values which occurred at the critical angle were determined [4, 5]. The earthquake motion at a specific point on the ground was recorded along two horizontal directions and one vertical direction. However, according to some studies, the vertical direction component of ground motion can be considered uncorrelated with the horizontal direction components [6]. When studies from the past right up to the present day are examined, many describe the effect of earthquake angles (2-directions) in engineering constructions [7-11]. In these studies, the structures were subjected to earthquake ground accelerations with values ranging from 0° to 90° and 0° to 180° in increments of 5, 6, 15, 20, and degrees [12-15]. However, earthquake motions exist not only 2-direction but also in 3-direction directions when determining earthquake behaviour in various engineering structures in many papers [16, 17]. A range of construction types are evaluated asymmetric-plan structures [18], a high-rise steel building [19], RCC (Reinforced Cement Concrete) frames [20], a highway tunnel [21], tuned liquid column dampers [22], RC bridge [23], skewed bridges retrofitted with buckling-restrained braces [24], masonry building [25], RC building [26], hybrid reinforced concrete-steel building [27], and these are analysed and designed with regard to different seismic excitation angles. When the results of these studies were examined, it was observed that the maximum earthquake forces acting on a structure can occur at different angles. It is of great importance that these maximum forces are considered during the dimensioning stage of a structure. Different sources of uncertainty exist when determining the direction of the ground motion in the seismic analysis of bridges.

Designers often do not know the direction in which predominant ground motion will occur at a bridge site. Many studies have been conducted to determine earthquake behaviours affecting bridges [28-36]. In Cronin's [37] thesis, the effect of the incidence angle on the nonlinear structural response of highway bridges was investigated through extensive statistical simulations. The time-history response of a 2D-SDOF system exposed to three sets of 40 ground motions was broadly analysed using linear elastic and elastic plastic springs by Bortoli et al. [38].

This study shows the effect of the earthquake angle on the structural behaviour of a concrete highway bridge. For comparison, 19 directions were considered, whose values ranged from 0° to 90°, each increasing by 5° in increments of 5°. The variations in the maximum displacements and internal forces on the deck, column, piles, and isolator were considered to determine their influence on the seismic performance. The results showed significant changes in the displacements, internal forces, and stresses. The maximum values occurred at different incident angles for each bridge member.

2. Ground motion incidence angle

To evaluate the influence of ground motion rotation, the two orthogonal (longitudinal and transverse) components of acceleration $\ddot{u}_{xg}(t)$ and $\ddot{u}_{yg}(t)$ were rotated by the regarded degree and resolved to the structural degrees of freedom (Figure 1.a). It was confirmed that üxg(t) and $\ddot{u}_{xg}(t)$ were initially oriented along the X (longitudinal) and Y (transverse) directions, respectively. The counter-clockwise rotation (θ) of ground motion components can be resolved to equivalent ground motion components along the axes ($\ddot{u}_{s1}(t)$ and $\ddot{u}_{s2}(t)$) of the structural degrees of freedom. $\ddot{u}_{zg}(t)$ and $\ddot{u}_{s3}(t)$ represent the vertical motions which are not affected by planar rotation.

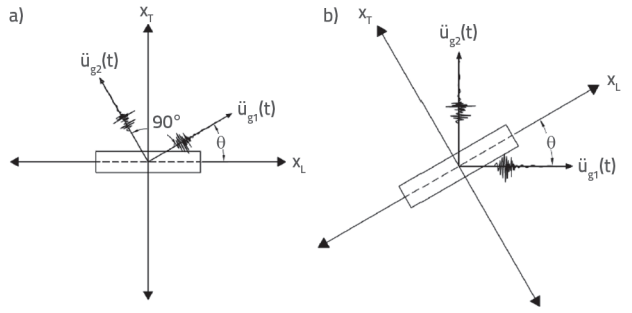

Figure 1. Rotation of ground motion: a) acceleration; b) structure

$$\ddot{u}_s = T \cdot \ddot{u}_g \tag{1}$$

$$\begin{bmatrix} \ddot{u}_{s1}(t) \\ \ddot{u}_{s2}(t) \\ \ddot{u}_{s3}(t) \end{bmatrix} = \begin{bmatrix} \cos\theta & -\sin\theta & 0 \\ \sin\theta & \cos\theta & 0 \\ 0 & 0 & 1 \end{bmatrix} \begin{bmatrix} \ddot{u}_{xg}(t) \\ \ddot{u}_{yg}(t) \\ \ddot{u}_{zg}(t) \end{bmatrix} \tag{2}$$

The transformation matrix (T) is used to perform this operation and is based solely on geometry [36]. Notably, the term üzg(t) shows the vertical motion, which is not affected by planar rotation.

A similar approach can be used to study the ground motion incidence angles [31, 39]. This rotates the structure and transforms the original ground motion components into rotated structural degrees of freedom (Figure 1b).

$$\ddot{u}_s = T_t \ddot{u}_g \tag{3}$$

$$\begin{bmatrix} \ddot{u}_{s1}(t) \\ \ddot{u}_{s2}(t) \\ \ddot{u}_{s3}(t) \end{bmatrix} = \begin{bmatrix} \cos\theta & -\sin\theta & 0 \\ -\sin\theta & \cos\theta & 0 \\ 0 & 0 & 1 \end{bmatrix} \begin{bmatrix} \ddot{u}_{xg}(t) \\ \ddot{u}_{yg}(t) \\ \ddot{u}_{zg}(t) \end{bmatrix} \tag{4}$$

The transformation matrix T_t is the inverse of T and can also be thought of as a clockwise rotation of the ground motion in terms of a stationary structure [37].

3. Description of bridge

The Gülburnu Highway Bridge which lies between 20+362 km and 20+692 km from the Giresun-Espiye state highway in Giresun, Turkey, was selected as a numerical example. The bridge is located in a landscape of considerable natural beauty, close to the port of Zefre, and spans Gulburnu Cove. Some views of the Gülburnu Highway Bridge are shown in Figure 2.

Finite element modelling of long-span highway bridges constructed using the balanced cantilever method is crucial for evaluating real structural responses. 2D or 3D finite element models can be constructed by considering different assumptions of the design criteria:

- The bridge deck and columns were modelled using frame elements.
- In the 2D finite element model, the section properties of each segment were calculated and assigned to the frame elements. Rigidity frame elements were used for distance connections.
- In the 3D finite element model, the non-prismatic section definition option was used to obtain the variable sections directly.
- Pre-stress and/or post-tension cables were modelled using frame elements constrained to the rotation and fixed to the end of each segment. The pre-stresses and/or post-tension loads were considered as strains.
- The boundary conditions at the ends of the deck and columns are defined using rigid springs and restraints.
- If any, the expansion joint in the middle of the bridge is modelled using a spring element to allow movement in the longitudinal direction.

The Gülburnu Highway Bridge was constructed with a balanced cantilever method using the cast-in-place construction technique because this is the best and optimum method for passing large and long valleys with reinforced concrete highway bridges using the maximum span and minimum piers. In this method, piers and a small part of the bridge deck are first constructed over a substructure using a suitable formwork.

The deck of the Gülburnu Highway Bridge, with its twin prestressed concrete box girder structures, consists of a 165 m main span and two 82.5 m side spans. The total length and width of the bridge were 330 m and 30 m,

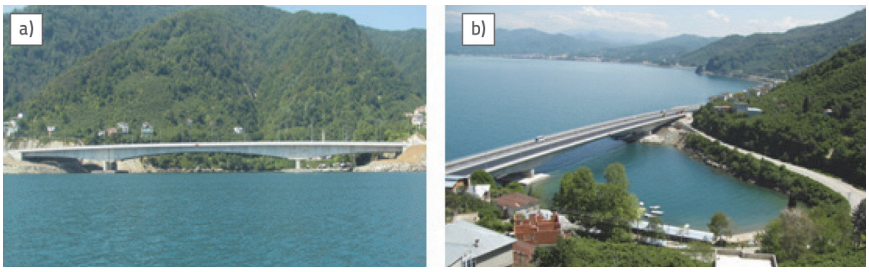

Figure 2. Some views of the Gülburnu Highway Bridge

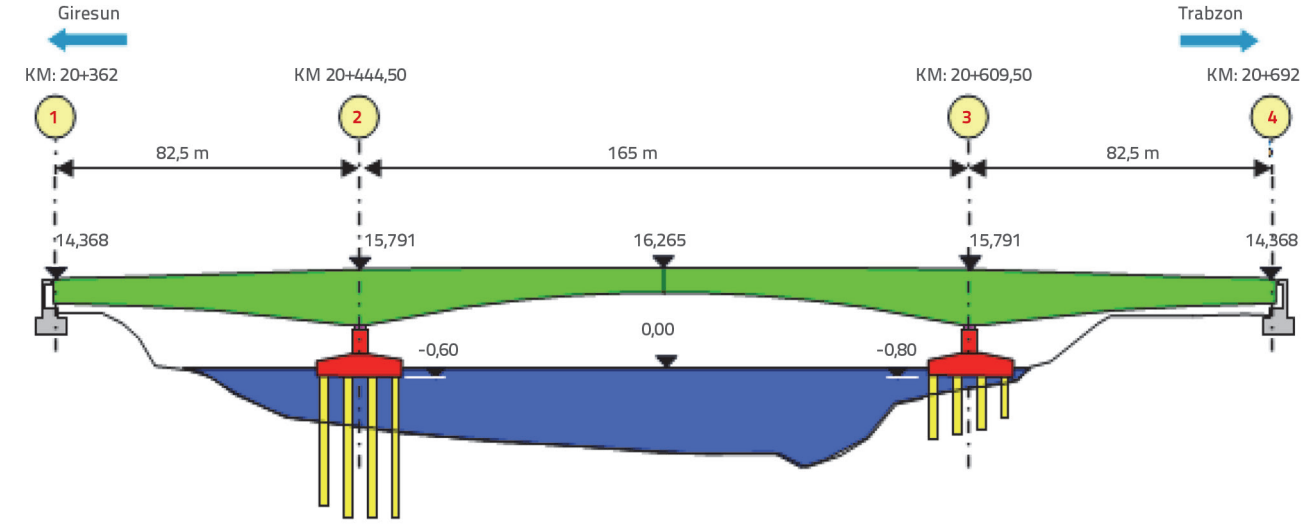

Figure 3. Basic configuration of Gülburnu Highway Bridge [40]

respectively. The basic configuration of the bridge is shown in Figure 3.

The bridge deck consists of 65 segments, which are approximately 5 m long and vary along the length of the bridge cross-section. The thickness of the bottom slab varied parabolically from 25 to 140 cm. A top slab with a thickness of 25 cm is fixed along the entire structure. The widths of the web elements varied from 45 to 60 cm. The designed strength of the concrete in the cast-in-place box girder segments was 40 MPa. The box girder deck was fully prestressed using tendons with a yield strength and 15.7 mm diameter. The number of tendons in the top slab, side abutments, and midpoint of the bridge varied between two, respectively. The number of tendons in the bottom slab varies from six to two along the piers from the abutments. There were thirty-four tendons in the middle of the bridge, decreasing to two along the piers. Figure 4 shows the dimensions of the box girder cross section.

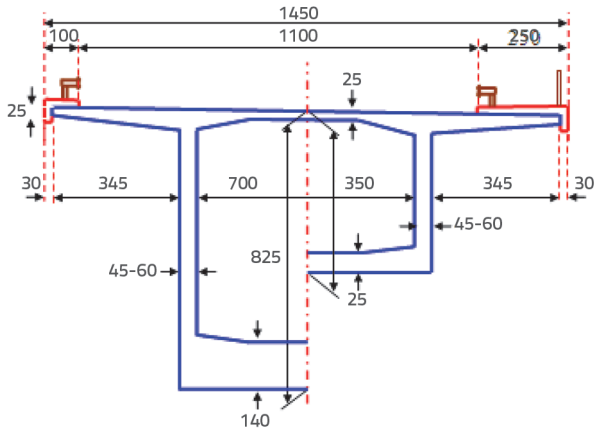

Figure 4. Dimensions of box girder cross-section (all dimensions are cm)

Four piers with a height of 4.50 m and a cross-sectional area of 9.00 x 3.75 m^2 exist on two raft foundations, each of which has dimensions of 32 x 22 m^2 and 3 m depth. There were twenty-eight bored piles, 200 cm in diameter and 25 m in length, on average. The design strengths of the concrete in the foundation and piles were 35 MPa and 30 MPa, and S420 reinforcement steel was used in the foundation. Figure 5 presents some views of the members of the bridge selected for finite element model analyses.

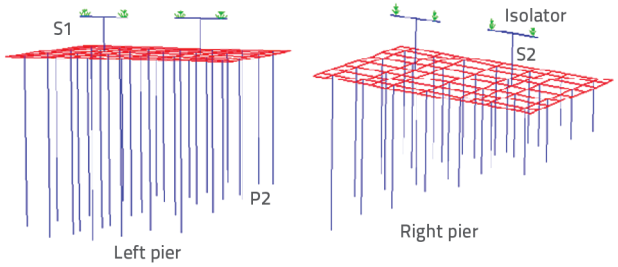

Figure 5. Views of the elements selected for analysis

4. Finite element analyses and analytical dynamic characteristics

The 3D finite element model of the bridge was modelled using SAP2000 [41] software. The deck, piers, and bored piles were modelled using frame elements with three translational DOFs and three rotational DOFs at each node. The raft foundations were modelled as shell elements. The abutments were modelled with limited boundary conditions which have freedom of longitudinal translation. The boundary conditions at the ends of the compressed piles were defined using rigid springs based on the values from the design project [42]. Figure 6 shows three-dimensional finite element model of the Gülburnu Highway Bridge. Table 1 lists the properties of the materials used in the analyses.

From the dimensional modal analyses of the bridge, eight natural frequencies were obtained analytically, ranging from 0-6 Hz. The first eight modes with 80 % of the modal participating mass ratios were selected. Analytical mode shapes can be classified into vertical, torsional, transverse, and longitudinal modes [40].

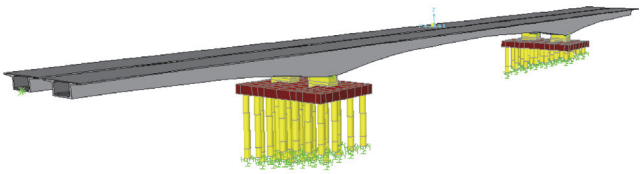

Figure 6. Finite element model of Gülburnu Highway Bridge

5. Seismic performance of the bridge

This study examines the seismic behaviour of bridges under different earthquake angles using seismic records from an

Table 1. Material properties considered in finite element analyses

Elements	Class	Modulus of elasticity [N/m²]	Poisson ratio [-]	Density [kg/m³]
Deck	C40	$3.4 \cdot 10^{10}$	0.2	2500
Piers	C35	$3.3 \cdot 10^{10}$	0.2	2500
Piles	C30	$3.2 \cdot 10^{10}$	0.2	2500
Foundation	C30	$3.2 \cdot 10^{10}$	0.2	2500
Steel*	S420	$2.1 \cdot 10^{11}$	0.3	7850
*Yield stress = 1600 MPa, Ultimate stress = 1860 MPa				

Table 2. Strong-motion records were selected for consideration

No	Near-fault strong ground motions					
	Earthquake	Component	Magnitude	Depth [km]	Site [*]	Peak ground acceleration
1	1992, Erzincan	NS	6.7	4.38	C-D	0.3869g
2	1992, Erzincan	EW				0.4961g
3	1992, Erzincan	UP				0.2345g
*Site: Local site classes (C and D soil groups)						

earthquake which caused loss of life and property in 1992 in Erzican, Turkey. ERZICAN/ERZ-NS, ERZICAN/ERZ-EW, and ERZICAN/ERZ-UP are the terms used for the components of the 1992 Erzincan earthquake, selected as the reference source for the ground motion records. Figure 7shows the time histories of the accelerations in the three directions in these records. Strong ground-motion records were obtained from the PEER Strong-Motion Database [43]. Table 2 presents information on the site conditions and soil types for the instrument locations in the ground motion records.

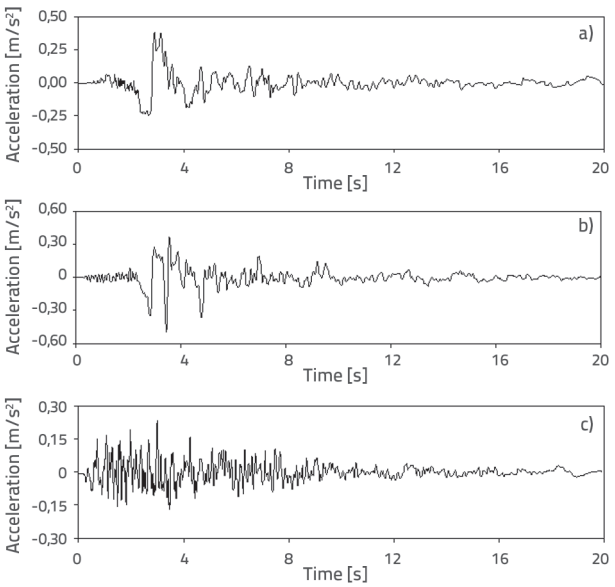

Figure 7. ERZICAN/ERZ acceleration component of the 1992 Erzincan earthquake: a) ERZICAN/ERZ-EW components; b) ERZICAN/ERZ-NS components; c) c) ERZICAN/ERZ-UP components

These records were simultaneously assigned to the x (longitudinal), y (transverse), and z (vertical) directions during analysis. In the first analysis, for 0° , the EW component was applied along the x direction, the NS component along the y direction, and the UP component along the z direction.

Figure 8 presents a flowchart of the seismic analyses for different earthquake angles. In this figure, the angle changes in the x- and y-directions are shown in yellow and green, respectively, such that they are perpendicular and equal to each other.

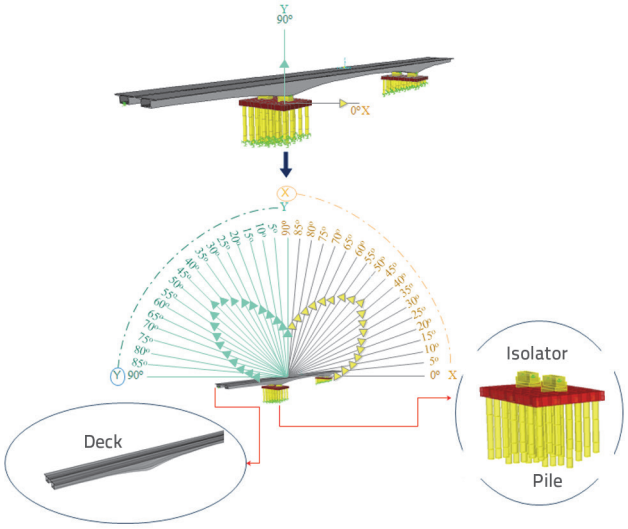

Figure 8. Flowchart of the seismic analyses at different earthquake angles

5.1. Displacements

5.1.1. Displacement of bridge deck

Nineteen earthquake angles ranging between 0° and 90° were applied, and the resulting displacements on the bridge deck were obtained. The angles of the earthquake directions were determined in 5-degree increments, perpendicular to each other.

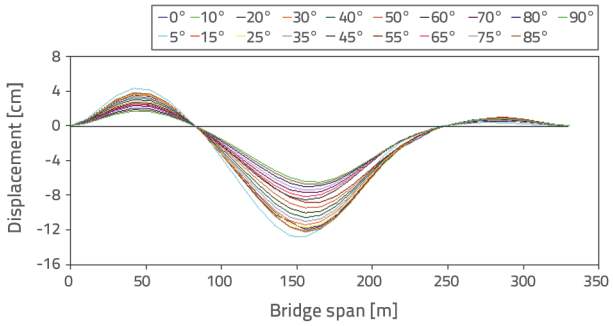

Figure 9. Changes in maximum vertical displacements along the bridge deck

Figure 9 shows the vertical displacements caused by angle changes at the deck. The maximum differences were calculated to

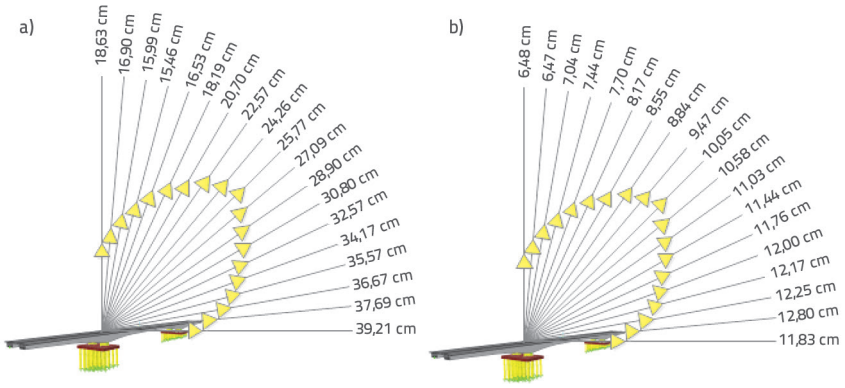

Figure 10. Maximum difference in displacement for each earthquake angle: a) X direction; b) Z direction

be 60.57 % and 49.45 % in the longitudinal and vertical directions, respectively. The maximum displacements in the longitudinal and vertical directions formed at each angle on the bridge deck are shown in Figure 10. It can be seen that the displacements of the longitudinal and vertical directions of the bridge deck were changed considerably with the changes in earthquake angle.

5.1.2. Displacement of the isolator and S2 column

Figure 11 shows the maximum X- and Y-direction displacements caused by the angle changes at the bridge isolator and top joint of S2 column.

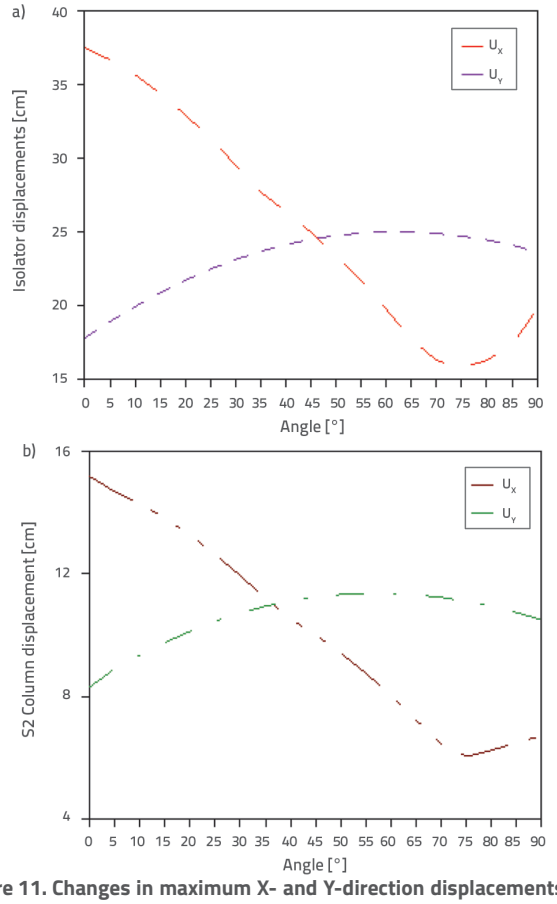

Figure 11. Changes in maximum X- and Y-direction displacements of bridge isolator and top joint of S2 column

The maximum differences were calculated as 58.07 % and 60.34 % for the longitudinal direction, and 40.57 % and 37.00 % for the transverse direction of the isolator and S2 column, respectively. Evidently, the displacements in the longitudinal and transverse directions of the bridge isolator and S2 column changed significantly with different earthquake angles.

5.2. Internal forces

5.2.1. Bridge deck

At the end of the analyses, Figure 12 shows the changes in the axial forces, shear forces, and maximum bending moments of the bridge deck. These results show that the axial forces, shear forces, and bending moments changed significantly by59.53 %, 26.78 %, and 50.09 %, respectively, for the bridge deck. The maximum differences in axial forces, shear forces, and bending moments formed at each angle on the bridge deck are shown in Figure 13.

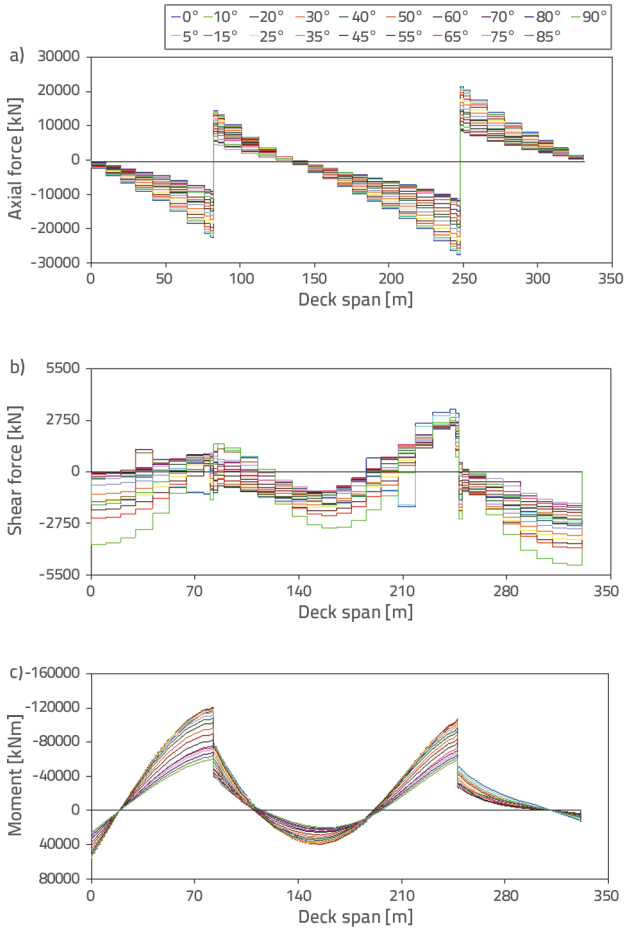

Figure 12. Changes in maximum axial forces, shear forces, and bending moments along the bridge deck: a) Axial forces; b) Shear forces; c) Moments

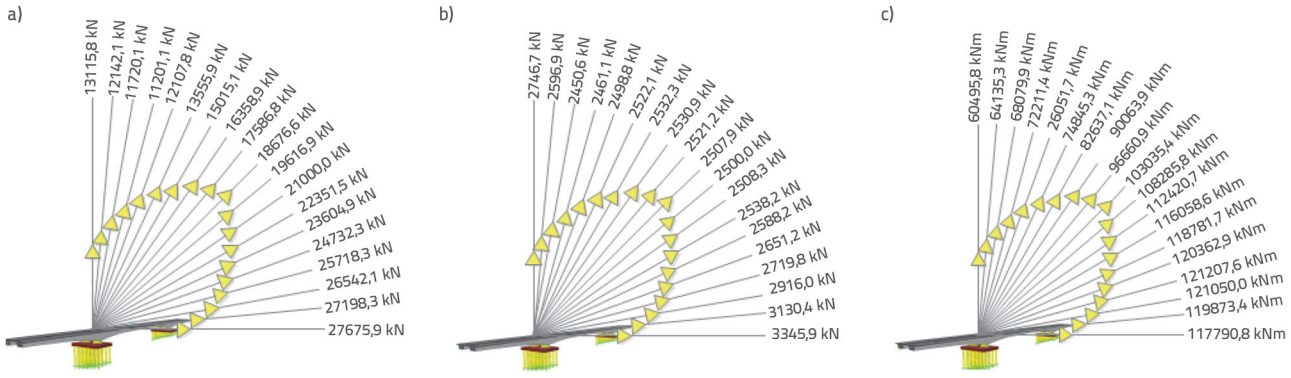

Figure 13. Maximum differences in internal forces for bridge deck span: a) maximum axial force; b) maximum shear force; c) maximum bending moment

5.2.2. S1 column

Figures 14.a, 15.a and 16.a show the changes in the axial, shear, and maximum bending moments of S1, respectively. These results indicate that the axial, shear, and bending moments changed significantly by 40.61 %, 165.51 %, and 132.07 %, respectively for S1 column. The time histories of the maximum and minimum axial forces, shear forces, and bending moments of S1 are shown in Figures 14.b, 15.b and 16.b, respectively.
Considering the maximum values in S1 column for different earthquake angles, it can be observed that the shear force and bending moment have very large differences. Achieving the maximum earthquake load by considering different angles in the project stage will be highly effective in terms of the dimensions.

5.2.3. P2 pile

Figures 17.a, 18.a and 19.a show the changes in the axial forces, shear forces, and maximum bending moments of P2 pile. These results indicate that the axial forces, shear forces, and bending moments changed significantly by51.28 %, 49.06 %, and 49.07 %, respectively for P2 pile. Figures 17.b, 18.b and 19.b show the time histories of the maximum and minimum axial forces, shear forces, and bending moments for P2 pile.

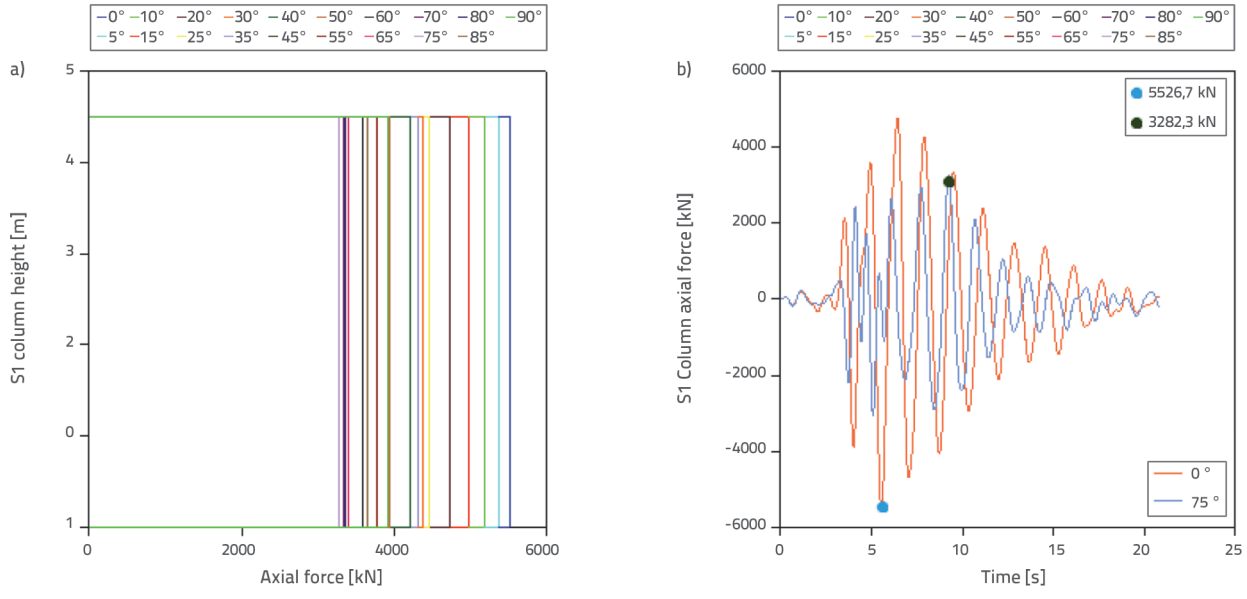

Figure 14. a) and b) changes in time histories of maximum axial forces along height of S1 column

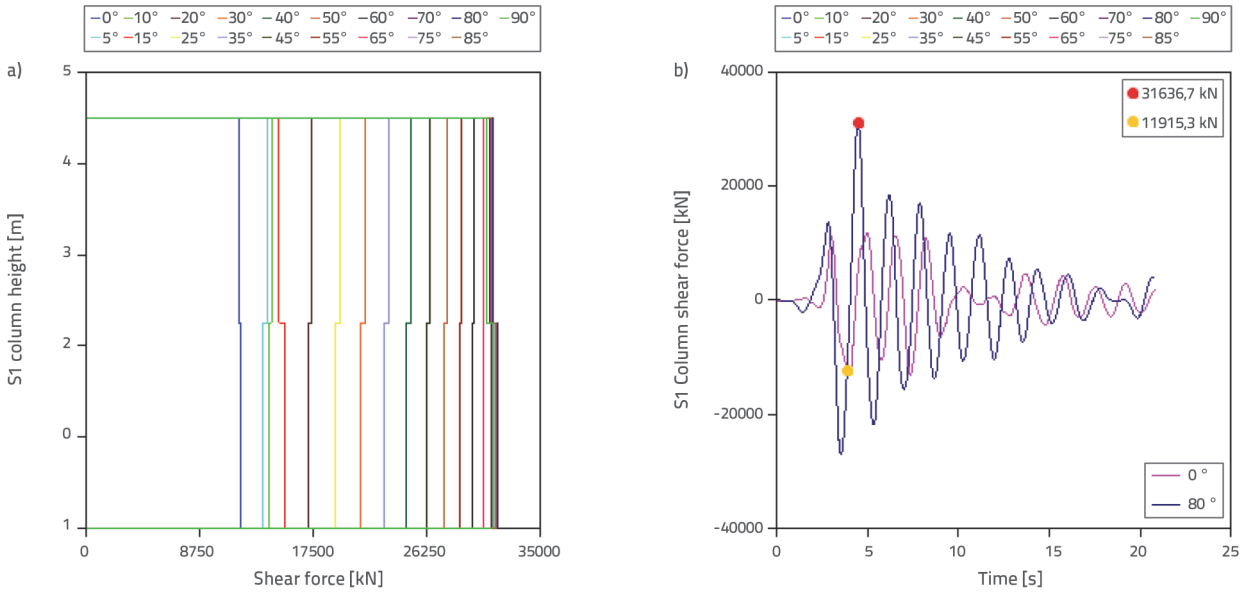

Figure 15. a) and b) Changes in time histories of maximum shear forces along height of S1 column

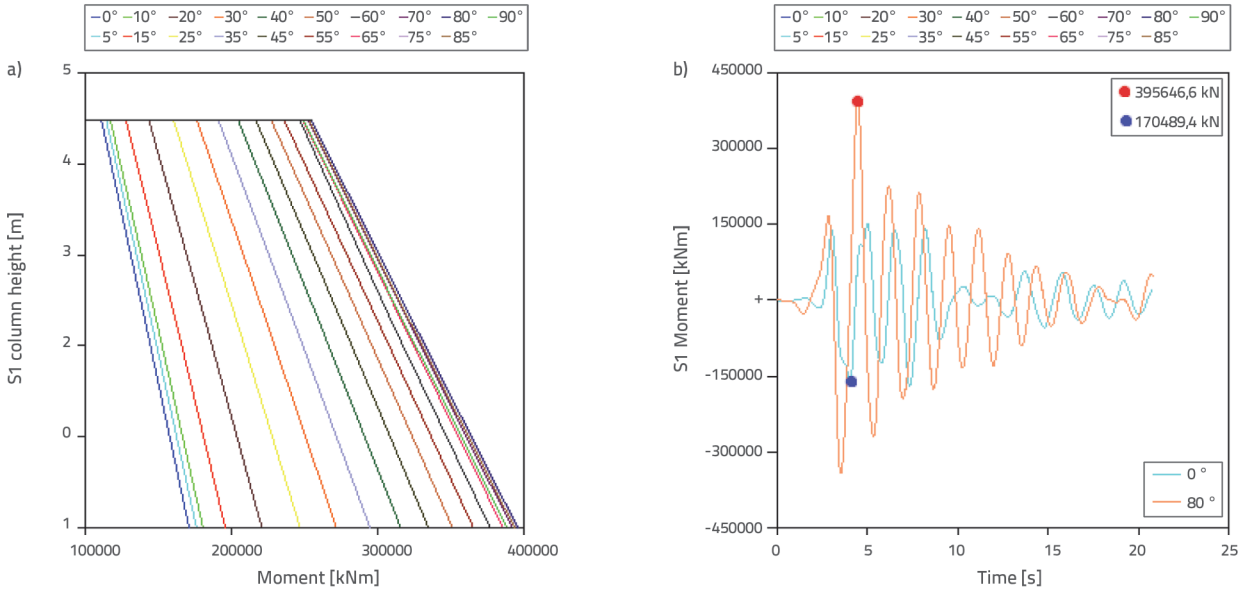

Figure 16. Changes in time histories of maximum bending moments along height of S1 column

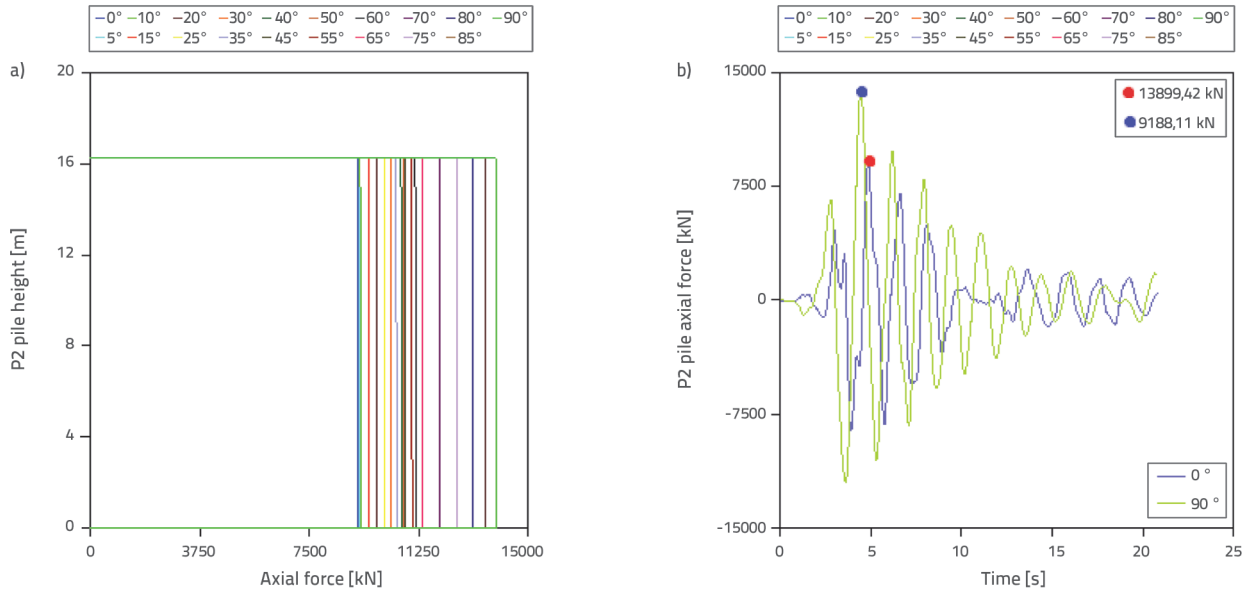

Figure 17. Changes in time histories of maximum axial forces along height of P2 pile

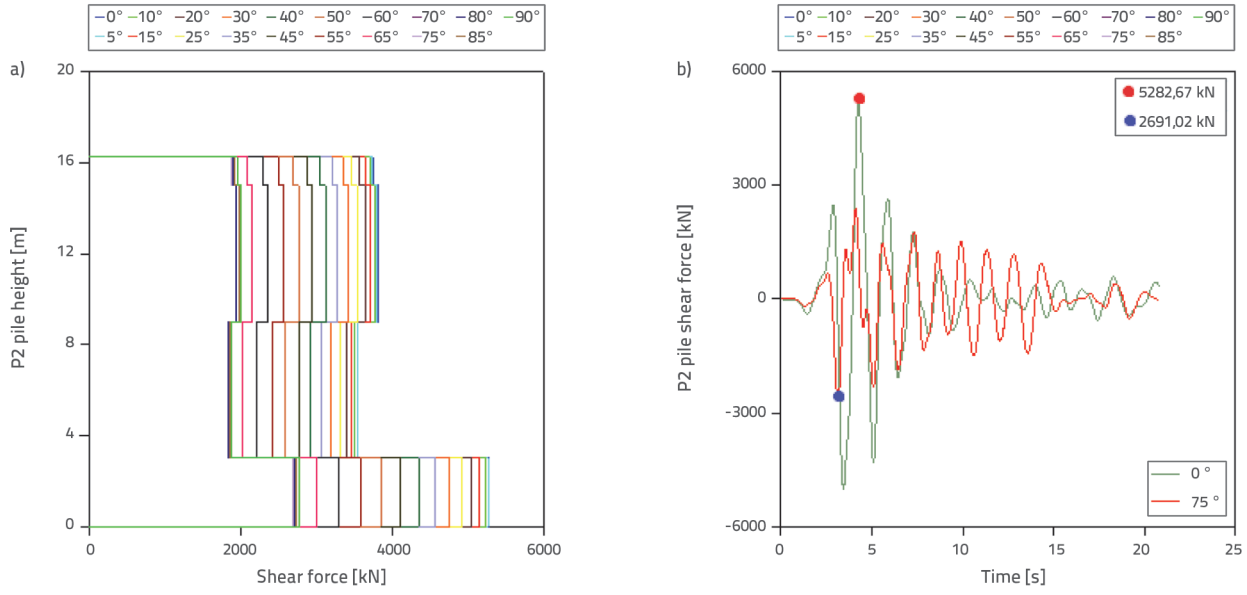

Figure 18. Changes in the P2 pile, and time histories of the maximum shear forces along its height

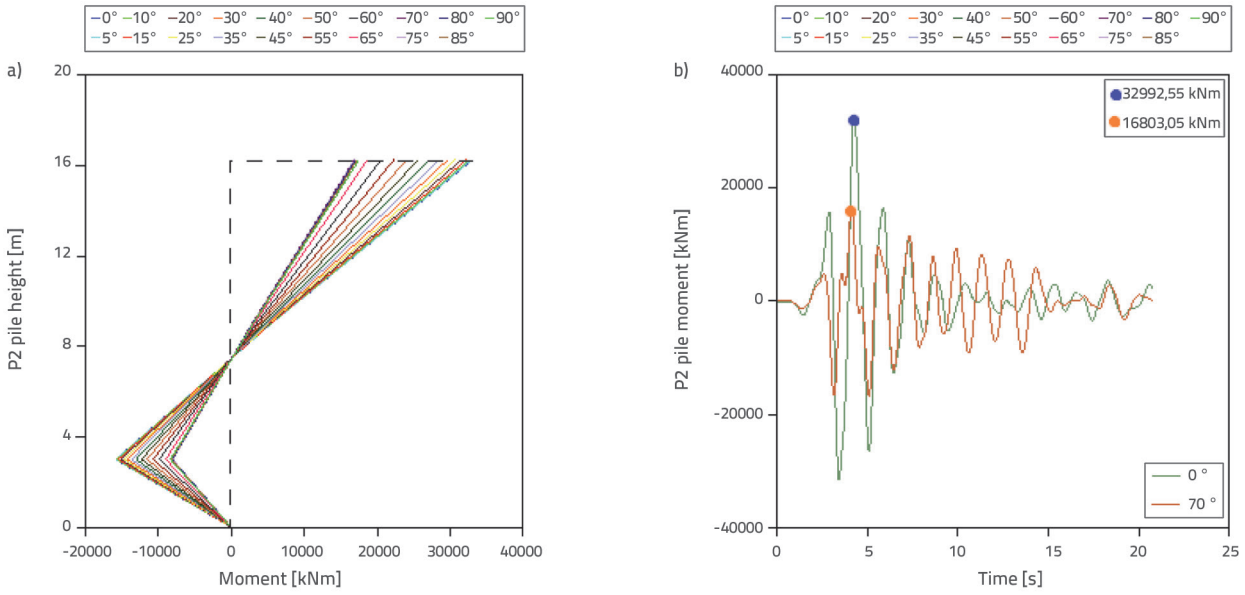

Figure 19. Changes in P2 pile, and time histories of the maximum bending moments along its height

5.3. Principal stresses

Figure 20 shows the maximum compressive and principal tensile stress contours obtained from the foundation at all earthquake angles.

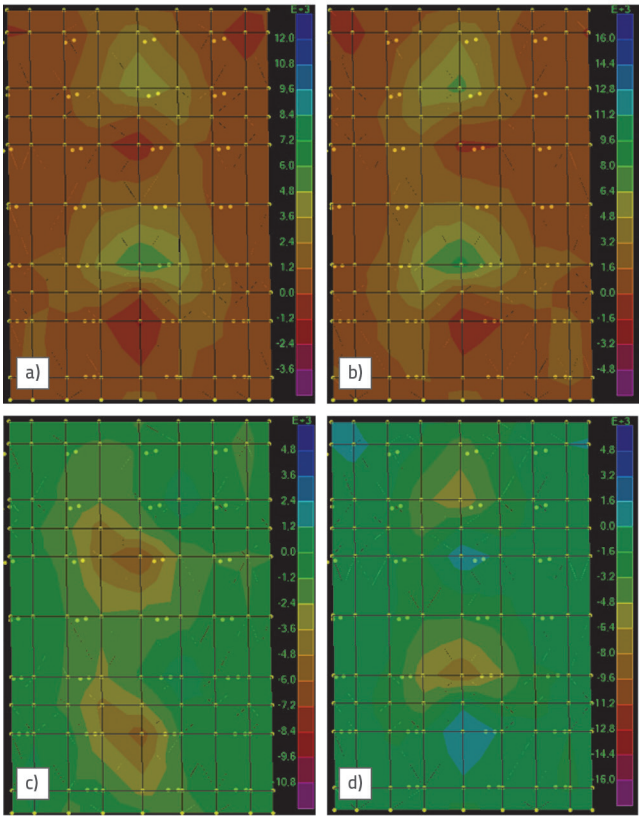

Figure 20. Maximum compressive-tensile principal stress contours for the left foot of bridge foundation

The stress contours represent the distribution of the peak values reached by the maximum stresses at each point within the section. The maximum and minimum tensile stresses were 15.742 MPa and 11.203 MPa at 90° and 0°, respectively (Figure 20.a to 20.b). Additionally, the maximum and minimum compressive stresses were obtained as 17.112 MPa and 11.692 MPa at 90° and 0°, respectively (Figure 20.c to 20.d). These results show that the tensile and compressive stresses changed significantly by 40.50 % and 46.36 %, respectively.

6. Conclusion

This paper presents an investigation into the influence of different earthquake angles on the seismic performance of a concrete highway bridge. For this purpose, a twin-prestressed concrete box-girder highway bridge was analysed using finite element methods. The bridge was subjected to the 1992 Erzincan earthquake ground accelerations in 19 directions, with values ranging between 0° and 90° and increasing in 5-degree increments.

From the modal analysis, eight natural frequencies were obtained, ranging from 0 to 6 Hz. Analytical mode shapes can be classified into vertical, torsional, transverse, and longitudinal modes. The horizontal and vertical displacements of the bridge changed considerably at different earthquake angles. The maximum differences were calculated as 60.57 % and 49.45 % in the X- and Z-directions, respectively. For the isolator and S2 column of the bridge, the maximum differences were calculated as 58.07 % and 60.34 % in the longitudinal direction and 40.57 % and 37.00 % in the transverse direction, respectively. The axial forces, shear forces, and bending moments changed significantly as follows:59.53 %, 26.78 %, and 50.09 % for the bridge deck; 40.61 %, 165.51 %, and 132.07 % for the S1 column; 46.71 %, 44.08 %, and 37.03 % for the P1 pile; and 51.28 %, 49.06

%, and 49.07 % for P2 pile. The tensile and compressive stresses varied between 40.50 % and 46.36 %, respectively.

The results of this study show significant changes in displacement, internal forces, and stresses. The maximum values occurred at different incident angles for each bridge member. No unique specific angle of incidence was observed for any structure. Therefore, using the maximum values obtained by considering the effective angle of each element in the dimensioning stage of the structural elements is highly effective for determining the dimensions of the structural element. In this study, it is recommended to use the maximum values obtained at different seismic angles for earthquake loads to be considered during the planning phase of new bridges. For existing bridges of strategic importance, the dimensions obtained by repeating earthquake analyses at different angles can be applied to structures with reinforcement studies.

REFERENCES

[1] Eurocode.: EN 1998-1-Eurocode 8: Design of Structures for Earthquake Resistance-Part I: General Rules, Seismic Actions and Rules for Buildings. [Authority: The European Union Per Regulation 305/2011. Directive 98/34/EC. Directive 2004/18/EC], 2004.

[2] FEMA, Building Seismic Safety Council for the Federal Emergency Management Agency; FEMA368-NEHRP, Recommended Provisions for Seismic Regulations for New Buildings and Other Structures. Washington. D.C., Building Seismic Safety Council, 2000.

[3] TERDC, Turkish earthquake resistant design code: Specifications for structures to be built in disaster areas, Ministry of Public Works and Settlement. General Directorate of Disaster Affairs. Earthquake Research Department. Ankara. Turkey. http://www.deprem.gov.tr, 2007.

[4] Athanatopoulou, A.M.: Critical orientation of three correlated seismic components, Eng. Struct., 27 (2005), pp. 301-312.

[5] Song, B., Pan, J.S., Liu, Q.: The study on critical angle to the seismic response of curved bridges based on pushover method, The 14th World Conference on Earthquake Engineering October, 12-17,China, 2008.

[6] Penzien, J., Watabe, M.: Characteristics of 3-d earthquake ground motions, Earthquake Engineering and Structural Dynamics, 3 (1975), pp. 365-373.

[7] Gonzalez, P.: Considering earthquake direction in seismic analysis Earthquake Engineering, Tenth World Conference, Balkema, Rotterdam, ISNB 9054100605, 1992.

[8] Rigato, A.B., Medina, R.A.: Influence of angle of incidence on seismic demands for inelastic single-story structures subjected to bidirectional ground motions. Engineering Structures, 29 (2007), pp. 2593-2601.

[9] Fujita, K. and Takewaki, I.: Critical correlation of bidirectional horizontal ground motions, Engineering Structure, 32 (2010) 1, pp. 261-272.

[10] Kostinakis, K.G., Athanatopoulou, A.M.: Evaluation of scalar structure-specific ground motion intensity measures for seismic response prediction of earthquake-resistant 3D buildings, Earthquakes and Structures, 9 (2015) 5, pp. 1091-1114.

[11] Altunışık, A.C., Kalkan, E.: Earthquake incidence angle influence on seismic performance of reinforced concrete buildings, Sigma Journal of Engineering and Natural Sciences, 35 (2017) 4, pp. 609-631.

[12] Lagaros, N.D.: Impact of the earthquake incident angle on the seismic loss estimation. Engineering Structures, 32 (2010), pp. 1577-1589.

[13] Lucchini, A., Monti, G., Kunnath, S.: Nonlinear response of two-way asymmetric single-story building under biaxial excitation, Journal of Structural Engineering, ASCE, 137 (2011) 1, pp. 34-40.

[14] Kumar, N.K., Gajjar, R.K.: Nonlinear response of two-way asymmetric multistory building under biaxial excitation, International J. Eng. Tech., 5 (2013) 2, pp. 1162-1168.

[15] Kanya, S., Rao, C.M.: Effect of earthquake incidence angle on seismic performance of RC buildings, International Journal of Research in Engineering and Technology, 4 (2015) 13, pp. 156-161.

[16] Fujita, K., Takewaki, I.: Property of critical excitation for moment-resisting frames subjected to horizontal and vertical simultaneous ground motion, Journal of Zhejiang University Science, 10 (2009) 11, pp. 1561-1572.

[17] Altunışık, A.C., Kalkan, E.: Investigation of earthquake angle effect on the seismic performance of steel bridges, Steel and Composite Structures, 22 (2016) 4,

[18] Nguyen, V.T., Kim, D.: Influence of incident angles of earthquakes on inelastic responses of asymmetric plan structures, Structural Engineering and Mechanics, 45 (2013) 3, pp. 373-389.

[19] Tun, M., Htun, Z.M.: Comparison of the effect of irregular high-rise steel buildings based on different seismic excitation angles, International Journal of Scientific Engineering and Technology Research, 3 (2014) 10, pp. 2252-2256.

[20] Quadri, S.A., Madhuri, M.N.: Investigation of the critical direction of seismic force for the analysis of RCC frames, International Journal of Civil Engineering and Technology, 5 (2014) 6, pp. 10-15.

[21] Sevim, B.: Assessment of 3D earthquake response of the Arhavi Highway Tunnel considering soil-structure interaction, Computers and Concrete, 11 (2013) 1, pp. 51-61.

[22] Altunişik, A.C., Yetişken, A., Kahya, V.: Experimental study on control performance of tuned liquid column dampers considering different excitation directions, Mechanical Systems and Signal Processing, 102 (2018), pp. 59-71.

[23] Tehrani, P., Ghanbari, R.: Investigating different methods for application of earthquake records in seismic evaluation of irregular RC bridges considering incident angles. Structures, 32 (2021), pp. 1717-1733.

[24] Wang, Y., Ibarra, L., Pantelides, C.: Effect of incidence angle on the seismic performance of skewed bridges retrofitted with buckling-restrained braces, Engineering Structures, 211 (2020), 110411.

[25] Liang, W., Xia, L., Zhu, Z., Mou, S., Zou, Zuyin, Yuan, S.: Torsional effect of the single-bay masonry building considering seismic wave incident angle, Structures, 44 (2022), pp. 1232-1246.

[26] Morfidis, K., Kostinakis, K.: Rapid Prediction of Seismic Incident Angle's Influence on the Damage Level of RC Buildings Using Artificial Neural Networks, Applied Sciences, 12, 3 (2022), p. 1055.

[27] Askouni, P.K.: The Behaviour of Hybrid Reinforced Concrete-Steel Buildings under Sequential Ground Excitations, Computation, 11, 5 (2023), pp. 102.

[28] Tseng, W.S., Penzien, J.: Seismic analysis of long multiple-span highway bridges, Earthquake Engineering and Structural Dynamics, 4 (1975), pp. 3-24.

[29] Zhu, D.S., Yu, L.S., Liu, S.Z.: The study of earthquake input principal direction for irregular bridges, Journal of Lanzhou Railway University, 19 (2000) 6, pp. 37-40.

[30] Armouti, N.S.: Transverse earthquake-induced forces in continuous bridges. Structural Engineering and Mechanics, 14 (2002) 6, pp. 733-738.

[31] Liang, Z., Lee, G.C.: Principal axes of m-DOF structures Part II: Dynamic loading, Earthquake Engineering and Engineering Vibration, 2 (2003) 1, pp. 39-50.

[32] Ateș, S., Soyluk, K., Dumanoğlu, A.A., Bayraktar, A.: Earthquake response of isolated cable-stayed bridges under spatially varying ground motions, Structural Engineering and Mechanics, 31 (2009) 6, pp. 639-662.

[33] Torbol, M., Shinozuka, M.: Effect of the angle of seismic incidence on the fragility curves of bridges, Earthquake Engineering and Structural Dynamics, 41 (2012), pp. 2111-2124.

[34] Atak, B., Avșar, Ö., Yakut, A.: Directional effect of the strong ground motion on the seismic behaviour of skewed bridges, Proceedings of the 9th International Conference on Structural Dynamics, Porto Portugal, 2014.

[35] Newton, B.: Understanding directionality concepts in seismic analysis. Memo to Designers, pp. 20-17, 2014.

[36] Ni, Y., Chen, J., Teng, H., Jiang, H.: Influence of earthquake input angle on seismic response of curved girder bridge Journal of Traffic and Transportation Engineering, 2 (2015) 4, pp. 233-241.

[37] Cronin, K.J.: Response sensitivity of highway bridges to random multi-component earthquake excitation, Master Thesis. University of Central Florida, Orlando, USA, 2007.

[38] Bortoli, M.D., Zareian, F., Shantz, T.: Significance of ground motion incidence angle in seismic design of bridges, National Conference on Earthquake Engineering, Frontiers of Earthquake Engineering, Anchorage, Alaska, 2014.

[39] Mohraz, B., Tiv, M.: Orientation of earthquake ground motion in computing response of structures Seismic Engineering, Pressure Vessels and Piping Conference, Minneapolis, USA, 195-202, 1994.

[40] Altunișık, A.C., Bayraktar, A., Sevim, B.: Output-only system identification of post tensioned segmental concrete highway bridges, J. Bridge Eng. ASCE, 16 (2011), pp. 259-266.

[41] SAP2000.: Integrated finite element analysis and design of structures, Computers and Structures Inc, Berkeley, California, USA, 2015.

[42] Yüksel Project: Gülburnu Bridge-detailed design, Ankara, Turkey 2007.

[43] PEER.: Pacific Earthquake Engineering Research Center, http://peer.berkeley.edu/smcat/data, 2016.